PHYSICAL REVIEW B **79**, 180402(R) (2009)

Phase locking of spin-torque oscillators by spin-wave interactions

Xi Chen*
School of Physics and Astronomy, University of Minnesota, Minneapolis, Minnesota 55455, USA

R. H. Victora†
Department of Electrical and Computer Engineering, University of Minnesota, Minneapolis, Minnesota 55455, USA

(Received 10 April 2009; published 5 May 2009)

The spin-wave mediated interaction leading to the phase locking of two spin-torque oscillators is studied. The effective coupling parameter is derived and unexpectedly found to exhibit an oscillatory behavior as a function of intercontact distance. The period of the oscillation is shown to equal the wavelength of the spin wave radiated from the contact. As a result, the oscillators will alternate between in-phase and out-of-phase oscillations, corresponding to maximal and minimal output powers. The predictions are confirmed by micromagnetic simulation.

DOI: 10.1103/PhysRevB.79.180402 PACS number(s): 75.30.Ds, 73.21.Ac, 72.10.Fk, 72.15.Lh

Angular momentum transferred from a spin-polarized electric current to the local magnetic moment gives rise to a spin transfer torque (STT) and opens up new routes for electrical manipulation of magnetization. Due to its applications in potential spintronic devices, the effect has stimulated many experimental and theoretical studies for the last decade.[1,2] Early theoretical work[1,3] predicts that spin waves (SWs) can be excited by electric currents, which has been observed in experiment.[4] On the other hand, when STT exactly cancels the intrinsic damping torque, a steady precession of local moment is produced. This is technologically attractive as a nanoscale microwave generator whose frequency can be tuned by the amplitude of the current.[5,6] It would be desirable to increase and direct the emitted microwave power. Recent experiments[7,8] in point contact geometry have demonstrated that two spin-torque oscillators (STOs) can be synchronized to increase the emission power. The mechanism of synchronization is attributed to spin waves, as shown in an elegant experiment.[9]

The SW assisted coupling between STOs is studied in recent theoretical work[10,11] by solving equations of motion for coupled nonlinear oscillators. In these simplified models, the spatial inhomogeneity of the SW is not taken into account explicitly. Instead, a phenomenological parameter is introduced to describe the coupling, whose physical meaning is yet to be clarified. Micromagnetic simulation has been carried out by Sano[12] in an attempt to elucidate the coupling mechanism beyond a model study. But the cell size (70×70 nm^2) used is so large compared to the SW wavelength that the dynamics of spatially nonuniform ($k\neq0$) SW modes is missed. By incorporating the inhomogeneity of the spin waves explicitly, we derive an expression for the coupling exhibiting an oscillatory behavior. The predictions are verified using micromagnetic simulation, where the cell size is adequately small (2 nm) to account for the full dynamics of SW excitations.

The model geometry used here is similar to experiment.[8] The structure contains two magnetic films, i.e., free and polarization layers, separated by a nonmagnetic spacer. The free layer is electrically connected to the electrode through two point contacts. The bottom polarization layer serves as the polarizer for the electric current. An external magnetic field is applied perpendicular to the film plane. In the calculation, we are only concerned with the dynamics of the free layer while assuming that the magnetization in the polarizing layer is fixed.

The dynamics is described using the Landau-Lifshitz-Gilbert (LLG) equation with spin-torque term included,[13]

$$\frac{\partial\hat{m}(x)}{\partial t}=-\gamma\hat{m}\times\vec{H}_{\mathrm{eff}}(x)+\alpha\hat{m}\times\frac{\partial\hat{m}}{\partial t}+\gamma H_{\mathrm{ST}}(x)\hat{m}\times(\hat{m}\times\hat{p}), \tag{1}$$

where $\hat{m}(x)$ is the directional vector of local magnetization, γ is the gyromagnetic ratio, α is the damping constant, $\hat{p}$ is the current polarization direction, and $H_{\mathrm{ST}}(x)=\frac{P\hbar j(x)}{edM_S}$ is the field induced by the spin current j, with thickness of free layer $d=5$ nm and polarization factor $P=0.25$. Permalloy $Ni_{80}Fe_{20}$ is used as the free layer with standard parameters $M_S=860$ emu/cm^3, $\alpha=0.02$, and exchange coupling $A=10^{-6}$ erg/cm.

Defining $m^{\pm}=m_x\pm im_y$ and $H^{\pm}_{\mathrm{eff}}=H_{\mathrm{eff}_x}\pm iH_{\mathrm{eff}_y}$, we can rewrite[14] the LLG equation (1) as follows:

$$i\frac{\partial m^+(x)}{\partial t}=\gamma m_z H^+_{\mathrm{eff}}-\gamma H_{\mathrm{eff}_z}m^+ + i\gamma H_{\mathrm{ST}}m_z m^+ + \alpha(\dot{m}_z m^+ - m_z\dot{m}^+). \tag{2}$$

The magnetic free energy takes the form: $E=\int[-M_S H_{\mathrm{ex}}\cdot m_z(\vec{x}) -2\pi[m_x^2(\vec{x})+m_y^2(\vec{x})]M_S^2+ A|\nabla\hat{m}(\vec{x})|^2]d\vec{x}$. The effective field $\vec{H}_{\mathrm{eff}}=(H_{\mathrm{ex}}-4\pi M_S m_z)\hat{z}+2\frac{A}{M_S}\nabla^2\hat{m}$ contains the out-of-plane external, demagnetization, and exchange fields.

Before considering the phase locking of double point contacts, we first study the case of a single contact in order to validate our model by reproducing established experimental results. For small amplitude oscillation with weak current, $m_z\approx1$ and Eq. (2) can be linearized as follows:

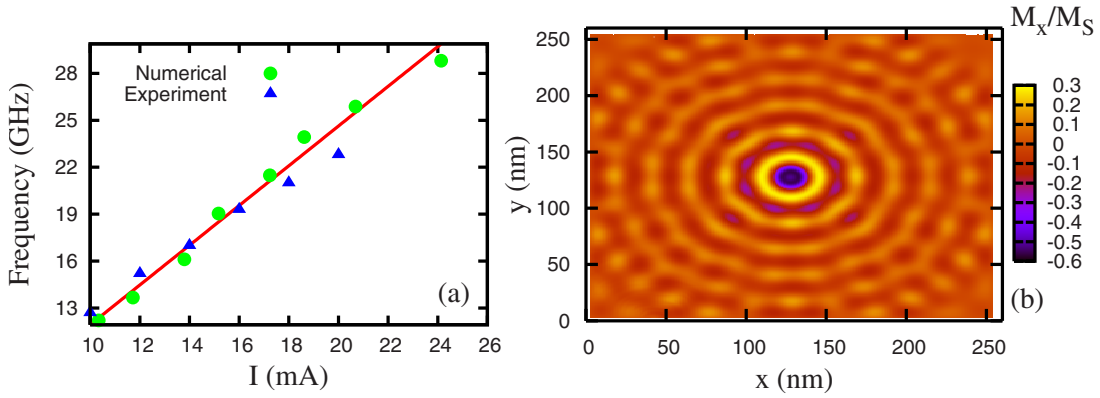

FIG. 1. (Color online) (a) Calculated dependence of peak frequency on current (circles) with a linear fit (solid line) and experimental results extracted from Ref. 16. (b) A snapshot of the steady-state SW configuration generated by the point contact.

$$\omega u = \frac{\gamma}{1 - i\alpha}\left(H_{\mathrm{ex}} - 4\pi M_S - \frac{2A}{M_S}\nabla^2 - iH_{\mathrm{ST}}\right)u, \tag{3}$$

where we assumed $m^+(x) = u(x)e^{i\omega t}$. One can solve Eq. (3) and obtain the propagating spin-wave solution $u(r) = cH_0^{(2)}(kr)$,[3] where k is the wave number, $H_0^{(2)}(x)$ is the Hankel function, and c is a constant to be determined.

To compare with experiment and visualize the SW solution $u(r)$, we solve the LLG equation with a single contact numerically. The micromagnetic simulation scheme follows the study of Dobin and Victora,[15] with the addition of a spin-torque term described in Eq. (1). The precession frequency is determined by the effective field perpendicular to the film plane. On the other hand, the z component of the demagnetization field can be tuned by the current density. Therefore frequency tunability can be realized by varying the current. Figure 1(a) shows the peak frequency's dependence on current as compared to the experiment,[16] where the contact diameter is 36 nm and a perpendicular external field $H_{\mathrm{ex}} = 1$ T is applied. We also calculated other experimental diameters and similar agreements are found. Both the experiment and calculation show a linear relation between current and frequency. The steady-state SW configuration excited by the point contact is shown in Fig. 1(b).

When two point contacts are placed on the same film, they interact through the propagating SW emitted from each other. The total energy can be expressed in terms of the superposition of the spin waves (m_1 and m_2) generated by two contacts, $E = \int\{-M_S H_{\mathrm{ex}} \cdot (m_{1z} + m_{2z}) + A|\nabla(\hat{m}_1 + \hat{m}_2)|^2 - 2\pi[(m_{1x} + m_{2x})^2 + (m_{1y} + m_{2y})^2]M_S^2\}d\vec{x}$. Therefore, the equation of motion for each STO is modified from Eq. (3) as follows:

$$-i\dot{m}_1^+ = \omega_1 m_1^+ - \left(\frac{\gamma}{1 - i\alpha}H_{\mathrm{ex}} - \omega_2\right)m_2^+ - i\dot{m}_2^+ = \omega_2 m_2^+ - \left(\frac{\gamma}{1 - i\alpha}H_{\mathrm{ex}} - \omega_1\right)m_1^+. \tag{4}$$

m_n^+ is assumed to follow the form of $m_n^+ = u_n(r)e^{i\phi_n}$ $(n = 1, 2)$. Rewriting Eq. (4) in terms of ϕ_n and subtracting the two equations, we obtain the equation of motion for the phase difference as follows:

$$\Delta\dot{\phi} = \Delta\omega - K\sqrt{1 + \left(\frac{\Delta K}{K}\right)^2}\sin(\Delta\phi + \delta), \tag{5}$$

where $\Delta\phi = \phi_2 - \phi_1$, $\Delta\omega = \omega_2 - \omega_1$, $K = \mathrm{Im}(f_2 + f_1)$, $\Delta K = \mathrm{Re}(f_2 - f_1)$, and $\delta = \arctan(\frac{\Delta K}{K})$ with $f_1 = (\frac{\gamma}{1-i\alpha}H_{\mathrm{ex}} - \omega_2)u_2(\mathbf{R_1})/u_1(\mathbf{R_1})$ and $f_2 = (\frac{\gamma}{1-i\alpha}H_{\mathrm{ex}} - \omega_1)u_1(\mathbf{R_2})/u_2(\mathbf{R_2})$. Using the solutions in Ref. 3, one can show that $f_1 \propto cH_0^{(2)}(k_1R_{12}) \overset{k_1R_{12}\gg 1}{\rightarrow} cR_{12}^{-1/2}e^{-ik_1R_{12}}$ and, similarly, $f_2 \overset{k_2R_{12}\gg 1}{\rightarrow} cR_{12}^{-1/2}e^{-ik_2R_{12}}$, where $\mathbf{R_n}$, ω_n, and k_n are the location, frequency, and wave number for STO n $(n = 1, 2)$. Therefore, K will exhibit sinusoidal oscillation as a function of separation between contacts R_{12}. Note that Eq. (5), known as Adler's equation,[17] is a quite general description for synchronization arising in various contexts such as electric circuits and Josephson junctions.[18]

An important prediction of Eq. (5) is that as we vary R_{12}, the two STOs will alternatively exhibit in phase, i.e., $\Delta\phi \approx 0$ for positive K, and out-of-phase oscillation, i.e., $\Delta\phi \approx \pi$ for negative K, with the period being the SW wavelength. This is manifested through the microwave power emitted from the sample. With in-phase oscillation, the wave emitted from the two STOs is added constructively; while in the out-of-phase case, they cancel each other leading to a vanishing emission power. Additionally, in the usual case of two phase-locked similar oscillators, ΔK will be small, $\Delta\dot{\phi} = 0$, and therefore

$$\sin\Delta\phi \approx \frac{\Delta\omega}{K}. \tag{6}$$

In the remainder of the Rapid Communication, we will carry out numerical calculation to verify these predictions. Experiments[7,8] have shown that there exists a phase-lock regime where two STOs with slightly different intrinsic frequencies synchronize. We first carry out simulation to reproduce the experimental observation. In the calculation, we place two contacts, with diameter 20 nm, 500 nm apart on a 704×704 nm^2 sample, with a perpendicular external field of 1.5 T. Additional damping is introduced on the boundary of sample in order to reduce spin-wave reflection, as suggested by Berkov *et al.*[19] The current through one contact is fixed at $I_1 = 4.5$ mA and I_2 is varied from 4.1 to 5 mA. The power

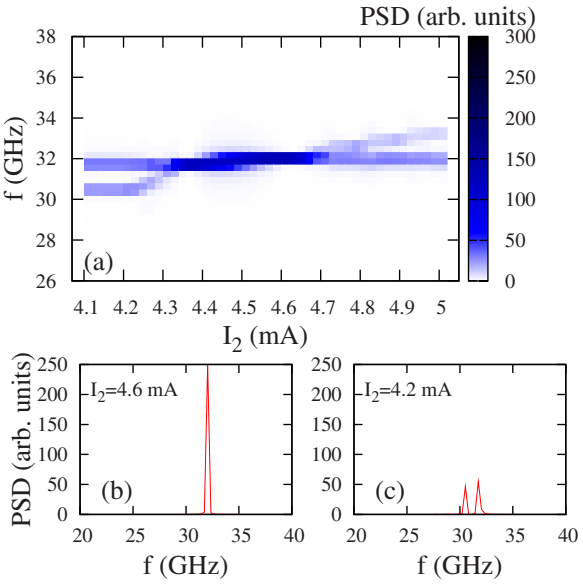

FIG. 2. (Color online) Phase lock of two STOs spaced at 500 nm. The current of one contact is fixed at $I_1=4.5$ mA, while I_2 is varied. (a) The map of PSD versus the frequency and I_2. (b) For $I_2=4.6$ mA, the two contacts are phase locked with a single peak and significantly larger output power. (c) For $I_2=4.2$ mA, the two contacts are not phase locked and two distinct peaks are shown.

spectral density (PSD), which is calculated from the square of the Fourier transform of the overall magnetization, is plotted in Fig. 2(a) as a function of I_2. Similar to experiment,[7,8] there exists a phase-locked region ($4.3<I_2<4.7$ mA) where the spectrum shows a single peak and the intensity is large. Outside this range, two distinct peaks are present and the power is significantly weaker. In particular, the spectrum for $I_2=4.6$ mA is shown in Fig. 2(b) within the phase-locked region, while for $I_2=5.0$ mA [Fig. 2(c)] two separate peaks are present indicating the absence of phase locking. It is also noticeable that the calculated results are quantitatively different from those observed in experiment.[7] In the present calculation, the two contacts are identical while, in experiment, the two ostensibly similar oscillators behave differently outside the phase-lock regime.

To confirm the prediction of oscillatory coupling between STOs, we vary the distance R_{12} with $I_1=4.5$ mA and $I_2=1.04I_1$. The two STOs are placed on the film symmetrically [for example, see Fig. 4(d)]. The combined PSD is shown in Fig. 3 as a function of frequency and distance from 60 nm to 220 nm. Though $I_1\neq I_2$, the two STOs are phase locked through out the whole range. The power oscillates with R_{12} with a period of about 34 nm, which agrees with the SW wavelength estimated from the dispersion relation.

In Figs. 4(a) and 4(b), we show the stationary phase difference $\sin\Delta\phi$ versus frequency difference $\Delta\omega$. Experimentally, $\Delta\phi$ can be measured by varying the phase between signals from two contacts using a phase shifter and observe the sinusoidal variation of the output power, as demonstrated in Ref. 7. The linear relation observed in Fig. 4 is consistent with Eq. (6), and the slope is the inverse coupling parameter $1/K$. When $R_{12}=100$ nm, the slope is positive leading to a positive K. In Fig. 4(b), the slope is reversed indicating a

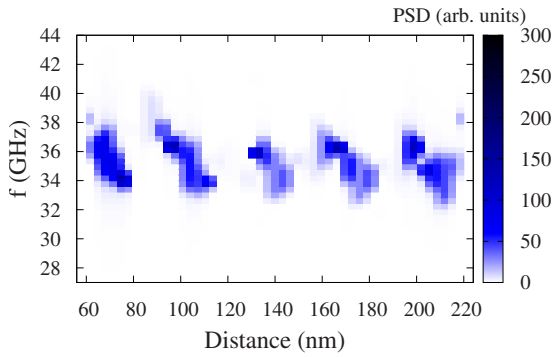

FIG. 3. (Color online) The map of combined power spectrum from both contacts versus frequency and distance R_{12}. The oscillation of output signal is caused by the oscillating coupling parameter $K(R_{12})$. The period is about 34 nm that matches the estimated SW wavelength.

negative K at $R_{12}=188$ nm. The SW configurations for these two cases are shown in Figs. 4(c) and 4(d). Furthermore, we calculate the coupling parameter K as a function of distance R_{12}. The results are plotted along with the analytic expression of K as previously defined in Fig. 4(e). The good agreement between simulation and theory in Fig. 4(e) demonstrates the validity of the effective equation of motion [Eq. (5)].

In order to detect the oscillating behavior of the coupling parameter, instead of varying R_{12}, one can alternatively fix R_{12} and vary k or the SW wavelength. Notice that the STO allows one to tune the frequency by changing the current;

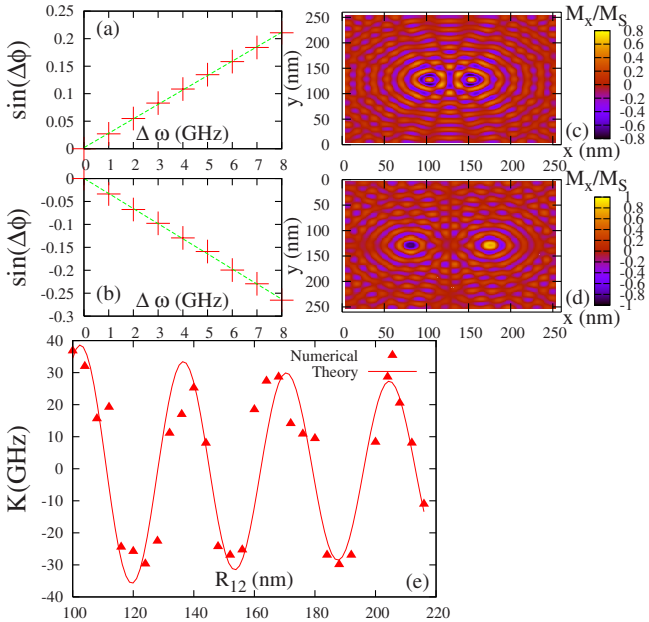

FIG. 4. (Color online) Calculated dependence of phase difference on frequency difference using Eq. (6) (line) and simulation (+) for (a) $R_{12}=100$ nm and (b)$R_{12}=188$ nm. Snapshot of the respective SW configuration shown in (c) and (d). (e) shows coupling parameter $K(R_{12})$ from simulation and theoretically evaluated using $K(R_{12})=\mathrm{Im}[(\frac{\gamma}{1-i\alpha}H_{\mathrm{ex}}-\omega_1)cH_0^{(2)}(k_1R_{12})+(\frac{\gamma}{1-i\alpha}H_{\mathrm{ex}}-\omega_2)cH_0^{(2)}(k_2R_{12})]$.

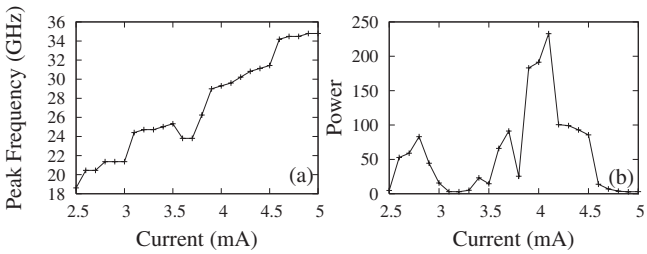

FIG. 5. Simultaneous variation in currents under both contacts while keeping $I_1=I_2$. (a) The blueshift of peak frequency with increasing current. (b) The variation in the integrated power.

and from the SW dispersion[3] relation $\omega=\gamma H_z(k)+\frac{\gamma A}{M_S}k^2$, the wavelength tuning can also be realized. Therefore one can change the coupling parameter as well as the output power by varying the current. This effect is displayed in Fig. 5(b), where the integrated power varies dramatically with current I while keeping $I=I_1=I_2$ and $R_{12}=200$ nm. A similar dependence of power on current is observed in Ref. 8. Additionally, the blueshift of peak frequency is shown in Fig. 5(a).

In the presented calculations, the Oersted field produced by the current is neglected to simplify the theoretical analysis. However, we have done calculations including the Oersted field and no qualitative difference is found. Hoeffer *et al.*[20] showed that application of an applied field at an angle to the surface normal can, in combination with the Oersted field, direct the spin waves so that one spin-torque oscillator receives a reduced number from the other. Our calculations show, however, that this second spin-torque oscillator will, in turn, radiate an increased number toward the first one, and thus our principle of coupling spin-torque oscillators through spin waves is preserved.

Another factor that affects the phase lock is the surface profile of the contact. The contact is not a pointlike object, and one cannot define a unique distance between two contacts. On the other hand, the coupling strength is sensitive to the distance. For a rough contact, the distance between two points on the contact fluctuates randomly; therefore, the coupling is averaged over a range determined by the roughness. In particular, when the roughness of the contact surface is comparable to the SW wavelength, our calculations show that the line width becomes wider and the coupling strength is weakened. These results will be discussed in more detail elsewhere.

In conclusion, the spin-wave mediated interaction between STOs is studied. The coupling parameter between the two STOs is derived using the equation of motion approach. Interestingly, the coupling parameter exhibits an oscillatory behavior versus the contact separation R_{12}, with the period equaling SW wavelength. As a consequence, the STOs will alternate between in-phase and out-of-phase oscillations, corresponding to maximal and minimal output powers. Numerical simulation is carried out and confirms this behavior. The analytic expression for coupling parameter is found to agree well with the numerical values. An alternative way to detect the effect by varying the currents under the two contacts is discussed.

This work was funded primarily by the National Science Foundation under Grant No. ECS-0621868, with partial support by MRSEC under Contract No. DMR-0212302. We also thank the University of Minnesota Supercomputing Institute for computer time and Yisong Zhang for valuable discussions.

*xichen@physics.umn.edu

†victora@ece.umn.edu

[1] L. Berger, Phys. Rev. B **54**, 9353 (1996).

[2] J. C. Slonczewski, J. Magn. Magn. Mater. **159**, L1 (1996).

[3] J. C. Slonczewski, J. Magn. Magn. Mater. **195**, 261 (1999).

[4] M. Tsoi, A. G. M. Jansen, J. Bass, W.-C. Chiang, M. Seck, V. Tsoi, and P. Wyder, Phys. Rev. Lett. **80**, 4281 (1998).

[5] S. I. Kiselev, J. C. Sankey, I. N. Krivorotov, N. C. Emley, R. J. Schoelkopf, R. A. Buhrman, and D. C. Ralph, Nature (London) **425**, 380 (2003).

[6] T. J. Silva and W. H. Rippard, J. Magn. Magn. Mater. **320**, 1260 (2008).

[7] S. Kaka, M. R. Pufall, W. H. Rippard, T. J. Silva, S. E. Russek, and J. A. Katine, Nature (London) **437**, 389 (2005).

[8] F. B. Mancoff, N. D. Rizzo, B. N. Engel, and S. Tehrani, Nature (London) **437**, 393 (2005).

[9] M. R. Pufall, W. H. Rippard, S. E. Russek, S. Kaka, and J. A. Katine, Phys. Rev. Lett. **97**, 087206 (2006).

[10] S. M. Rezende, F. M. de Aguiar, R. L. Rodriguez-Suarez, and A. Azevedo, Phys. Rev. Lett. **98**, 087202 (2007).

[11] A. N. Slavin and V. S. Tiberkevich, Phys. Rev. B **74**, 104401 (2006).

[12] E. Sano, Jpn. J. Appl. Phys., Part 2 **46**, L1123 (2007).

[13] S. Zhang and Z. Li, Phys. Rev. Lett. **93**, 127204 (2004).

[14] M. A. Hoefer, M. J. Ablowitz, B. Ilan, M. R. Pufall, and T. J. Silva, Phys. Rev. Lett. **95**, 267206 (2005).

[15] A. Y. Dobin and R. H. Victora, Phys. Rev. Lett. **90**, 167203 (2003).

[16] F. B. Mancoff, N. D. Rizzo, B. N. Engel, and S. Tehrani, Appl. Phys. Lett. **88**, 112507 (2006).

[17] R. Adler, Proc. IEEE **61**, 1380 (1973).

[18] K. Wiesenfeld, P. Colet, and S. H. Strogatz, Phys. Rev. Lett. **76**, 404 (1996).

[19] D. Berkov and J. Miltat, J. Magn. Magn. Mater. **320**, 1238 (2008).

[20] M. A. Hoefer, T. J. Silva, and M. D. Stiles, Phys. Rev. B **77**, 144401 (2008).